





Right Place, Right Time!

Towards ObjectNav for Non-Stationary Goals

Vishnu Sashank Dorbala^{*1}  Bhrij Patel^{*1}  Amrit Singh Bedi²  and Dinesh Manocha¹ 

University of Maryland, College Park MD 20740, USA

Abstract. We present a novel approach to tackle the ObjectNav task for *non-stationary* and potentially occluded targets in an indoor environment. We refer to this task *Portable ObjectNav* (or P-ObjectNav), and in this work, present its formulation, feasibility, and a navigation benchmark using a novel memory-enhanced LLM-based policy. In contrast to ObjNav where target object locations are fixed for each episode, P-ObjectNav tackles the challenging case where the target objects move *during* the episode. This adds a layer of time-sensitivity to the navigation scheme, and is particularly relevant in scenarios where the agent needs to find portable targets (e.g. misplaced *wallets*) in human-centric environments. A P-ObjectNav agent needs to estimate not just the correct location of an object, but also the time at which the object is at that location for visual grounding — raising a question about the feasibility of this task. We address this concern by studying two cases for object placement: one where the objects placed follow a routine or a path, and the other where they are placed at random. We *dynamize* Matterport3D for these experiments, and modify PPO and LLM-based navigation policies for evaluation. Using PPO, we observe that agent performance in the random case stagnates, while the agent in the routine-following environment continues to improve, allowing us to infer that P-ObjectNav is solvable in environments with routine-following object placement. Further, using memory-enhancement on an LLM-based policy, we set a benchmark for P-ObjectNav. The memory-enhanced agent significantly outperforms non-memory based counterparts across object placement scenarios by 71.76% and 74.68% on average when measured by Success Rate (SR) and Success Rate weighted by Path Length (SRPL), showing the influence of memory on the improving the performance of a P-ObjectNav agent. Our code and dataset for object placement will be made publicly available for reproducibility.

Keywords: Embodied AI · Large-Language Models · Object Navigation

1 Introduction

We present an approach to tackle Object Navigation (ObjectNav) in dynamic scenarios with non-stationary targets. While embodied tasks including ObjectNav [3, 40, 49], ImageNav [12, 26, 48], PointNav [15, 41, 52] and even Audio-Guided

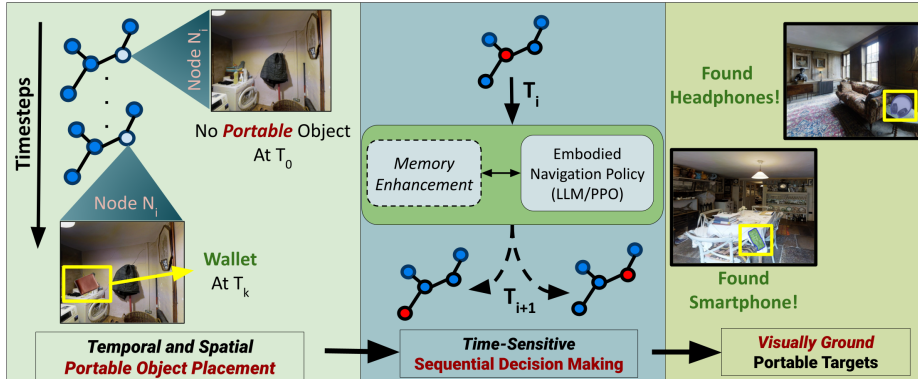


Fig. 1: We present a new approach to tackle ObjectNav with non-stationary and potentially occluded target objects by defining the **P-ObjectNav** task. We first *dynamize* scans from the Matterport3D [7] dataset, by placing portable objects to images corresponding to their natural rooms at various times (eg. *wallet* in *office* between timesteps 1-25 in the image above). We then perform navigation on this modified dataset and set a benchmark using a *memory-enhanced* LLM agent. Beyond temporal changes in placement, our dataset also introduces occlusions and spatial transformations for added realism, which we study using SoTA object detectors.

navigation [8, 9] have been studied in *static* environments [18, 21, 39, 41], their adoption to dynamic scenarios with moving goals has been limited. In this work, we present an approach to tackle such dynamic scenarios by formulating the **Portable Object Navigation** (P-ObjectNav) task, which requires an agent to consider environmental changes for path planning and visually identifying *non-stationary* targets.

Recent developments in Embodied AI have led to the emergence of several unique navigation challenges that rely on of various forms of perception. In ObjectNav for instance, an agent is tasked with navigating to an instance of a specified target object class, such as “couch” or “fridge”, relying on visual object grounding [28, 32] to know if it has reached its goal. However, these tasks often assume static environments, neglecting the dynamic nature of the real world where objects can move and need not be entirely visible.

Navigation in dynamic environments has been typically limited to *low-level* planning tasks such as crowd avoidance [4, 34, 43] and socially aware navigation [6, 33], where an agent actively performs real-time maneuvers to find a path that is smooth and collision-free while trying to minimize time. On the other hand, *high-level* planning is less time-sensitive and usually involves sequential decision-making using percepts obtained from waypoints or nodes on a topological graph [10, 45] to reach a target destination. Literature on the combined case of high-level planning in dynamic environments with non-stationary targets has been scarce to non-existent.

Performing this kind of high-level navigation in dynamic environments is particularly relevant in household scenarios involving finding small objects that a user tends to misplace. For instance, if a user routinely leaves their glasses

in the garage, an agent tasked with finding them needs an estimate of not just *where* the glasses are, but also *when* the glasses are usually there. Analogous to Chatbots that provide personalized assistance based on historical data [27], a P-ObjectNav agent must be able to identify user behaviors over time in a dynamically changing environment to make personalized decisions on locating a target object.

In defining such non-stationary target objects, a natural question arises regarding the feasibility of P-ObjectNav. Much akin to an endless game of hide and seek, if objects are constantly being moved, would an agent ever be able to find any target? In low-level planning, this falls under the pursuit-evader class [1, 46] of problems. In a high-level planning task however, such situations are for the most part left unaddressed. As such, we first seek to prove feasibility, by comparing agent performance in *random* and *routine-following* object placement scenarios. An agent placed in a routine following scenario must intuitively show continuous improvement in finding portable targets over an agent attempting to find targets that are randomly placed.

We then present a novel memory-enhanced approach to tackle ObjectNav in non-stationary environments i.e., the P-ObjectNav task. Figure 1 presents an overview of our approach.

Main Results. Our work makes the following key contributions:

- We develop a novel approach to tackle ObjectNav in scenarios with non-stationary and potentially occluded target objects. As part of our approach, we formulate the ***Portable ObjectNav*** task, establish its feasibility, and set a navigational benchmark using a novel memory-enhanced LLM-based policy. To the best of our knowledge, we are the first to tackle ObjectNav in this setup.
- We customize the Matterport3D dataset to accommodate the *dynamic* nature of our task by placing portable objects following both *temporal* and *positional* placement strategies. We will be releasing this dataset to promote research in this area.
- We establish the feasibility of P-ObjectNav by comparing performance of a PPO-agent in *random* and *routine-based* temporal object placement scenarios. Continuous improvement in the routine case over sporadic performance in the random case demonstrates the viability of our task in scenarios involving an *orderly* placement of target objects.
- Finally, we set a baseline for the P-ObjectNav task employing memory-enhancement an LLM-based agent, highlighting a drastic performance improvement of over 70% when measured across Success Rate (SR) and Success Rate Weighted by Path Length (SRPL).

2 Related Works

2.1 Embodied Navigation

Recent developments in Embodied Simulators [7, 16, 36, 37, 44] and subsequent works [3, 5, 30, 38, 41, 50] have established ObjectNav as a popular task in the

community. These also include zero-shot approaches that employ various foundation models [18, 20, 21, 57]. However, ObjectNav has predominantly been done in static environments, with fixed targets. While Habitat 3.0 [36] introduces the Social Rearrangement task, this is a human-robot teaming task where the agent is expected to rearrange objects in the house in tandem with the human. Our work deals strictly with a passive human case, where the agent is expected to find a non-stationary target without human assistance.

Planning in non-stationary environments has been studied in the past [35, 47, 58], with recent approaches even utilizing LLMs in conjunction with multi-arm bandits [14]. These schemes usually propose memory augmentations with hierarchical planning procedures and frame the problem from an obstacle avoidance standpoint [29, 47, 55]. In contrast, our work considers the case where the target itself is non-stationary.

Rudra et. al in [42] define small portable objects around the house, and propose a contextual bandit scheme that aims to learn the likelihood of finding an object at various waypoints. In their case,, however, object locations are shuffled only after each episode, meaning it finally boils down to an ObjectNav task in a static environment. In contrast, we tackle a *truly* dynamic case, where objects are moving even *during* the episode. This definition adds a layer of complexity as the embodied agent must now navigate towards a constantly shifting target object, for which it needs to identify specific routines and object movement patterns in the environment.

2.2 Visual-Language Grounding

An important component of ObjectNav is the object detection module that allows the embodied agent to perceive and understand the household scene. Object detection and semantic segmentation datasets like MS-COCO [31], ImageNet-2K [17], and LVIS [23] have brought great strides in pre-training visual models for everyday items. Furthermore, recent developments in vision foundation models [25, 28, 53] have allowed for zero-shot object detection and segmentation in household environments. With the advent of LLMs, a lot of new approaches for Object Navigation, especially in zero-shot conditions [18, 19, 21, 22, 51, 56] that rely solely on commonsense knowledge or LLM planning capabilities have garnered much interest. In our work, we adopt one of these approaches, LGX, and enhance it with memory to set a benchmark for P-ObjectNav.

3 P-ObjectNav: Task Overview & Approach

In this section, we first formalize the P-ObjectNav task and establish conditions for determining feasibility. We then discuss our environment setup as a modification of Matterport3D with various temporal and positional object placement strategies. Finally, we describe our PPO and LLM-based navigation policies and set a memory-enhanced benchmark.

3.1 Formulation

P-ObjectNav tackles ObjectNav in a constantly changing dynamic environment, with non-stationary target objects. This setting introduces a unique challenge for the agent that needs it to be at the right place, at the right time to successfully ground a target object. The agent in each episode is tasked with finding as many portable target objects as it can.

While the object positions are non-stationary, we hypothesize that the *object routes* need to be constant for an agent to learn patterns for successful task completion. We consider this constancy in object routes to be representative of human habits as routines [13]. As such, a P-ObjectNav agent aims to optimize,

$$\pi^* = \arg \max_{\pi} P(o_p | \pi(t), t) \quad (1)$$

where π is the agent's policy, which maximizes the probability of intersecting with a portable object o_p at time t and location $l = \pi(t)$.

In our case, we consider a high-level planning problem, requiring the agent to make decisions at nodes on a topological graph. To maximize the number of objects found within an episode or n timesteps, the agent's subgraph of sequential decision-making nodes i.e., $G_i(t_n)$ at trial i over n timesteps must maximize the intersection with the ground truth portable object subgraph over that time period $G'(t_n)$. The optimal subgraph $G_o(t_n)$ for n timesteps could be expressed as,

$$G_o(t) = \arg \max_{G_i(t), i \in \{1, \dots, I\}} |G_i(t) \cap G'(t)| \quad (2)$$

$$I = f(N_a, n)$$

Here, I represents the total number of possibilities or trials for a subgraph to evolve over n timesteps from a particular starting point N_a . Given the time constraint, I is finite on an undirected graph, meaning a solution for G_o must exist. However, if $G'(t)$ is not constant for each trial, G_o would keep varying.

Thus, when objects are placed according to a fixed *routine*, as the ground truth portable object subgraph $G'(t)$ remains constant during each trial in $G_i(t)$, an optimal policy is learnable over a set of trials. Conversely, if objects are moved at *random* without any underlying pattern, the environment becomes completely non-stationary from the perspective of the agent, and $G'(t)$ would change for each trial in $G_i(t)$, i.e, maximizing the variance of $G_o(t)$. This scenario nullifies the agent's ability to learn beyond mere chance. As such, to prove feasibility, we need to experimentally prove our theoretical assumption that -

$$\lim_{t \rightarrow \infty} (R_{routine}(t) - R_{random}(t)) \gg 0 \quad (3)$$

where $R_{routine}$ represents the agent's performance in a routine following environment, and R_{random} represents performance when P-Object motions are random. We hypothesize that over time, an agent performing P-ObjectNav in a routine-following environment should perform much better than an agent placed in a random environment.

Toward this objective, we conduct P-ObjectNav experiments in a *dynamized* Matterport3D environments using both PPO-based and LLM-based decision-making agents.

3.2 Object Placement

ObjectNav can be considered as a fusion of two components, i.e., *Sequential Decision Making* pertaining to the agent’s high-level navigation scheme, and *Visual-Language Grounding* which deals with the identifying the location of the target object from an image. To setup ObjectNav in a dynamic scenario, we associate object placement complexities in terms of **Temporal** and **Positional** placement with both these components.

Room	Portable Objects
Bedroom	Charger, Water Bottle, Smartwatch, Laptop, Notebook, Toothbrush, Mug, USB Flash Drive, Phone, Headphones, Hat
Garage	Screwdriver, Flashlight, Mug, Phone, Headphones, Hat
Dining	Salt and Pepper Shakers, Portable Speaker, Charger, Water Bottle, Mug, Bowl, Phone, Headphones, Hat
Office	Charger, Laptop, Hat, Notebook, USB Flash Drive, Mug, Phone, Headphones
Bathroom	Toothbrush, Phone, First-Aid Kit
Kitchen	Salt and Pepper Shakers, Hat, Mug, Bowl, Phone, Headphones, First-Aid Kit
Lounge	Playing Cards, Mug, Portable Speaker, Charger, Water Bottle, Laptop, Phone, USB Flash Drive, Dice, Headphones, Hat
Gym	Dumbbells, Jumprope, Smartwatch, Phone, Headphones, Hat
Outdoor	Jumprope, Smartwatch, Portable Speaker, Phone, Water Bottle, Headphones, Hat
Recreation	Playing Cards, Dice, Water Bottle, Headphones, Hat

Table 1: Rooms and Portable Objects: We map 21 portable objects to a set of rooms available in our Matterport3D scans. This mapping is used to set object locations during our Routine-based movement schemes. During each episode, the objects are placed in different rooms during for a range of timesteps. Commonly moved objects such as *phone*, *headphones*, *hat* are associated with 9 different rooms, while less commonly shifted ones such as *dumbbells* appear only in the Gym. The frequency of portable objects ranges from 1 – 9.

Given the computational overhead of existing simulators, we chose to modify Matterport3D [7] and make it *dynamic* for our task. This setup allows us to treat P-ObjectNav as a high-level sequential decision-making problem in which

the agent needs to determine the right sequence of discrete node “hops” to reach the portable target.

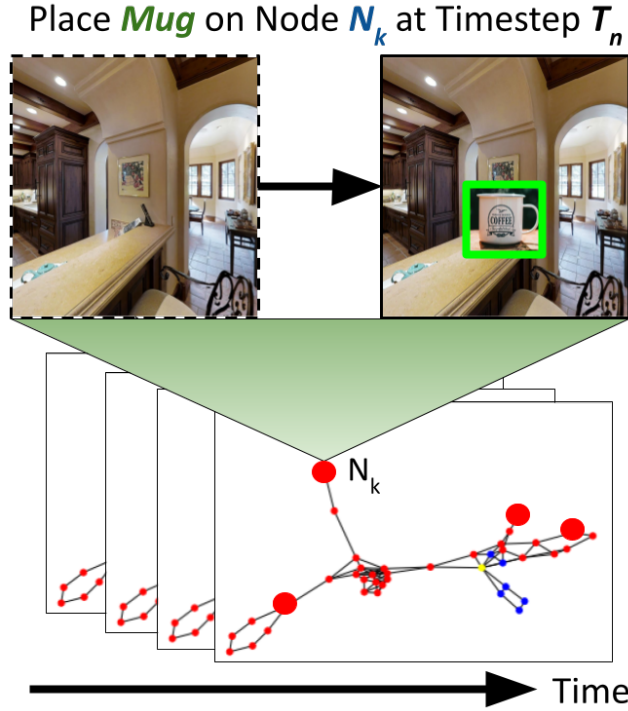


Fig. 2: Object Placement: Portable objects are placed at various timesteps on different nodes in the Matterport scan. As the agent explores the environment, the portable object keeps shifting positions. Here, the portable object *mug* is placed on a kitchen node N_k at time T_n . If the agent reaches the kitchen before T_n , it would fail to see the portable object.

We consider a set of 10 randomly chosen scans from Matterport3D [7] for experimentation. Each house scan contains topological graphs consisting of nodes representing panoramic images of the scene, and edges representing the distance between them. Additionally, each node contains information about the room type. We use these room types to obtain a mapping of portable objects, listed in Table 1. This mapping is used to determine routine movements described below.

Temporal Placement To introduce dynamism in the *Sequential Decision Making* described earlier, we modify the Matterport3D dataset to place portable objects on various nodes at different timesteps. This is illustrated in figure 2.

We compute trajectories of the portable objects in an offline manner. For each portable object, we compute a random partition of timesteps T . To emulate

realism, each object has a *waiting period*, w , where once it moves to a new location, it will wait there for a certain number of timesteps before being able to move again. Therefore, each element in T has at least w elements. For each element in T , we assign a room for the portable object to be in during those timesteps. The room is determined by a given object movement scheme that we detail below. Note that the new location chosen could also be the same location the portable object is in currently, i.e., the object can stay where it was.

We look at three forms of object movement schemes for our feasibility study:

1. **Random Movement:** As a baseline, we consider the case where portable object placement is completely random, in random rooms at random times. Their locations do not follow the mapping listed in Table 1.
2. **Semi-Routine Movement:** Portable object locations in this case are in accordance to the mapping, but the timesteps of placement remain variable between episodes. For instance, a toothbrush will move only between the bedroom and bathroom, but the time during which it moves would change between episodes.
3. **Fully-Routine Movement:** In this case, objects follow a specific placement pattern or a path that remains constant from episode to episode. For instance, a toothbrush in the bathroom during timesteps t_1 - t_2 would remain there at that time during all episodes.

Spatial Placement To introduce dynamism in the form of *Visual-Language Grounding* for P-ObjectNav, we consider spatial transformations and occlusions on the target objects. This is illustrated in figure 3.

We use FastSAM [54] to obtain segmentation masks for both the scene and the portable target object. For the scene segmentations, we filter out a set of k largest segments below the center of the image, to avoid placing target objects on ceilings. We then place the target objects on a randomly chosen segment from this set. This allows for spatial variance, allowing us to evaluate grounding approaches against various backgrounds. We also add occlusion, by cutting off a percentage of the target segment and pasting it on the scene segmentations. More details about this are in the supplementary.

3.3 Navigation Policies

We develop two embodied navigation agents for P-ObjectNav as follows:

PPO: We train the PPO agent for 2000 episodes with 50 timesteps per episode. In each episode, the task is to find the most amount of portable objects. The episode ends when either the agent has found all portable objects or it has exceeded the time limit.

For the observation space, the agent is given an $(n + 1)$ -dimensional vector where n is the number of nodes in the Matterport3D scan. Each element except for the last one, contains a binary value where the value is only 1 if the node corresponding to that index is adjacent to the current and is 0 otherwise. The

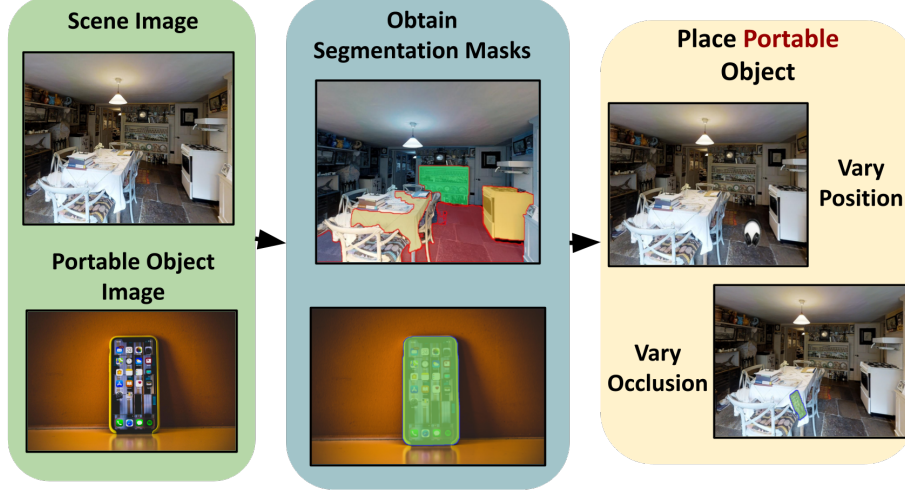


Fig. 3: Spatial Placement: To introduce dynamism in terms of visual-language grounding of the target, we consider various positions, orientations and occlusions of the target object in the scene. Given images of the scene and a stock image of the portable target object, we obtain segmentation masks from both. The target object is then placed onto the scene such that it stays above of segmentations below the center of the image. To mimic occlusions, we cut-off varying percentages of the of the target segmentation during the overlay.

last element in the observation space is the timestep. The action space is an integer representing the index of the node in the observation space input vector the agent will travel to next.

For each transition, the agent receives the following rewards:

- For each transition in the environment, the agent receives a reward of +1 for every new portable object from Table 1 it finds.
- If the action a is an index corresponding to a node that is not adjacent to the current node, the agent receives a penalty of -1.

Formally, let A be the set of adjacent nodes at timestep t , and let $P(t)$ be the set of new portable objects seen at t .

$$R(t) = |P(t)| - \mathbb{1}_{a \notin A} \quad (1)$$

We analyze the PPO training in Section 4 to highlight the feasibility of learning portable object trajectories when using a routine-based object movement-scheme as opposed to a fully random scheme.

LLM-Based: We implement LGX [18], an LLM-based SOTA model for zero-shot ObjectNav. Given a target object, at each timestep, LGX takes a list of objects around the agent and asks an LLM (GPT) to predict a target to navigate towards. The agent continues to do this till it has found the target.

In our implementation, we slightly modify LGX to our dynamic Matterport3D environment. At each timestep, we pass YOLO v8 [24] to obtain a list of objects in the scene, and then prompt GPT-4 with the object list asking for an object prediction from the list that might lead to a portable object. We then use the scene graph from Matterport3D to hop to the next node.

Memory Enhancement: Given the need to finetune agent behaviour to a specific object placement routine, we enhance LGX with memory by passing historical actions and timesteps to the prompt across trials. We do this in two ways -

1. **Complete:** Here, we pass in all the objects in view as well as the current GPT prediction to the system prompt of the agent. As the token size of GPT is limited to 4096 tokens, we maintain a horizon, where we remove the earliest appended observation when an overflow of tokens occurs.
2. **Selective:** Rather than passing the entire action history of the agent, we perform *memory selection* by utilizing a memory tree. During each timestep, we update the memory tree with the observations of the agent as well as the prediction that GPT makes. We then check if a path exists on the tree from the current node to a set of seen observations containing a portable object. If a path does exist, we prompt the LLM with the cost of travelling to that node, asking if it wants to backtrack, and if so, execute the traceback.

4 Experimentation & Results

We decouple the navigation and target grounding performance in our experiments. This separation allows us to better analyze the performance of each module.

4.1 PPO Training

Figure 4 shows the training curves between two PPO agents, one that trained on semi-routine portable object movement and another trained on random movement. The plots show that the agent trained on semi-routine movement was able to learn and improve performance, while the agent trained on random movement had no signal to learn from. For ease of training and proof of feasibility, we consider only 10 portable objects across 53 nodes of a single scan.

We monitor the number of *unique* objects that the agent has found across episodes on the graph on the left, while we monitor the cumulative reward per episode on the graph on the right of Figure 4. Note the improved performance of semi-routine agent over the random agent, while the fully routine agent seems to perform much worse. In order to analyze this better, we draw statistics about the nodes and objects that the agent views.

In figure 5, the graph on the left shows the area covered by each node on average during each episode, as well as the total unique area covered across all episodes. While all the agents explore lesser as time progresses, notice the extremely low coverage of the agent in the fully-routine environment, due to it's

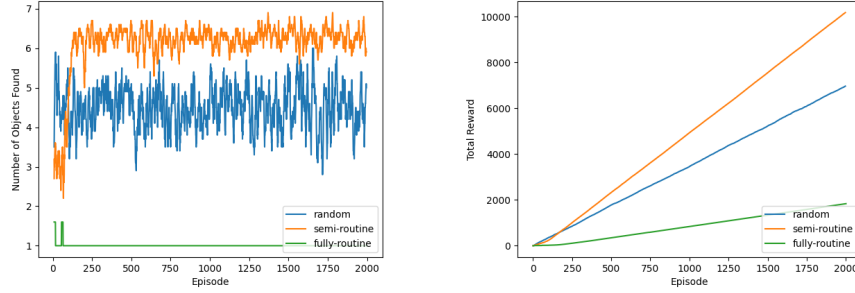


Fig. 4: Training curves for PPO agents trained on semi-routine (orange) and random movement (blue). **(Left)** The number of portable objects found at each episode. At max, 11 objects can be found. **(Right)** The total rewards up until the end of each episode. The semi-routine converges to a higher number of objects and rewards per episode than random movement which corresponds to humans leaving things with no habits.

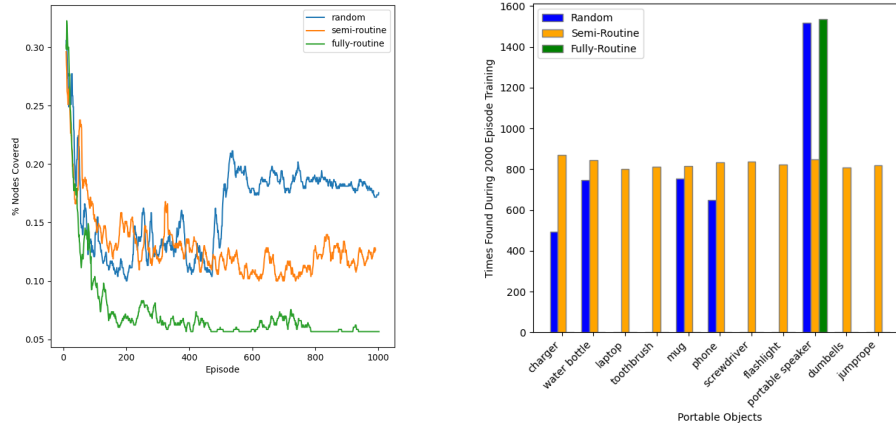


Fig. 5: Statistics on the PPO agents trained. **(Left)** Node coverage by each agent as a percentage of the total number of nodes (i.e., 53 in the test scan). **(Right)** Object-wise finding frequency. Note the uniform distribution in the semi-routine case, the *camping* behavior in the fully-routine case, and the sporadic behavior in the random case.

camping nature. The graph on the right shows a object-wise frequency distribution of the total number of objects found during the entire period of training. We observe that the fully routine agent tends to *camp* at one location where the *portable speaker* is at (which also has a larger waiting time w). This negatively affects its overall performance and explains the reward curve shown in as shown in Figure 4.

While the camping behaviour for the fully-routine case is not ideal, the agent placed in the semi-routine environment shows continuous improvement as suggested by its cumulative reward. This result is in line with our formulation presented earlier, and suggests the need for an orderly placement of objects where the locations are fixed, but not the timesteps for ideal learnability. The performance of the semi-routine following agent also satisfies our initial hypothesis introduced in equations 2 and 3 from the formulation section 3.1. We can thus experimentally infer that P-ObjectNav is feasible in environments with routine-based object placement that has a soft constraint on time, but a hard constraint on position.

4.2 LLM Inference

We evaluate our LLM based policies using two metrics, adapted from the original ObjectNav task.

- **Success Rate (SR)** represents the average success across all trials, and is a raw measure of portable object finding success. This is the number of episodes where a portable object was found in each trial, divided by the total number of timesteps, averaged across all trials. It is defined as -

$$SR = \frac{100}{\text{Num. Trials}} * \Sigma \frac{\text{Suc. Ep.}}{\text{Total Ep.}}$$

- **Success Rate Weighted By Path Length (SRPL)** is defined similar to SPL for ObjectNav [2], but is a comparative metric. It is defined as the success rate divided by the path length (or number of steps). As the number of steps taken is usually much larger than the success rate, we take the log of the step count, and the percentage of this value. It is represented as -

$$SRPL = 100 * \frac{SR}{\log(\text{Path Length})}$$

As we expect a high SR, and from a low number of steps, a higher value is preferred from this metric.

Table 2 presents the results of LGX on the P-ObjectNav task. We run the agent for 10 trials of a modified Matterport3D scan, with each trial having 20 episodes and 30 timesteps.

We make some salient observations. First, the memory enhanced agents perform significantly better on average compared to agents without memory. This is evident, as a LGX’s zero-shot performance is reliant on commonsense knowledge from GPT for decision making, which might not capture personalized object routines.

Second, LGX with Complete Memory performs much worse than LGX with Selective memory. As such, passing raw memory without any selectivity does not necessarily give good results. This can be attributed to an “input overload”

Policy	Object Placement	SR (%) \uparrow	SRPL (%) \uparrow
LGX	Random	4.12	0.45
	Semi-Routine	2.96	0.34
	Fully-Routine	7.14	0.82
LGX + Complete Memory	Random	5.45	0.74
	Semi-Routine	13.08	2.40
	Fully-Routine	11.53	1.38
LGX + Selective Memory	Random	7.00	0.93
	Semi-Routine	25.24	2.97
	Fully-Routine	20.95	2.46

Table 2: Evaluation of P-ObjectNav Policies Across Different Scenarios: We conduct experiments with agents with and without memory on the 3 different object placement scenarios described in section 4. We experiment with two types of memory, complete where we pass the entire list of observations, and selective, where we only pass relevant nodes when a path to a portable object exists. Note the overall improved performance of the selective memory enhanced agent across all object placement scenarios. Further, observe that the semi-routine scenario gives us best results overall. We attribute this to fully-routine scenarios being overly strict in terms of orderly placement for time and location.

where the LLM’s output is not desirable since it does not have a direct path to a portable object from the data it has been given.

Third, in using LGX with Selective Memory, the Semi-Routine object placement gives us the best results overall. The Semi-Routine case considers a soft constraint on the target’s time of placement allowing it to be moved at any time during the episode, while the location of the target is fixed to a set of rooms. This is an interesting result, which we can attribute to this case being a middle ground between aggressive (random) and conservative (fully-routine) placement behaviors. We infer that the fully-routine case is too strict, since the agent might be in the vicinity of a portable object, i.e., the right room, but might not find it due to it being at the wrong node in the room.

Finally, we notice that performance of the memory-enhanced agent in routine based placement scenarios is far superior than the agent in a random placement scenario. We can infer from this that memory is a strong component of what makes a successful P-ObjectNav agent. Unlike ObjectNav, where the fixed nature of object locations over time allows for agents to rely on commonsense reasoning for path planning, P-ObjectNav performance is not commonsense driven, but instead sensitive to memory. In the selective case, our agent uses a Memory Tree to store observations, and returns a path to the agent only when it exists. As such, we perform a *compression* of memory via our memory tree, which is interfaced to the LLM prompt. In the complete case, all previous observations are passed to the agent, giving it temporal data to reason about where to go next. The inclusion of memory allows for agents to store specific object placement patterns in the environment, allowing for improved inference over time.

5 Conclusion

We present an approach to tackle the ObjectNav task with non-stationary target objects. In extending ObjectNav, our approach formulates a new task called Portable ObjectNav or P-ObjectNav, defining conditions for its feasibility. In our experiment setup, we first customize a Matterport3D environment with non-stationary portable objects, simulating “dynamic” behavior by introducing temporal and spatial complexities. Our setup considers three cases, two of which involve objects being placed in a routine-following manner, and the other where objects are randomly moved around. Our results with a PPO-based agent on our Matterport3D environment show that over time, the performance of an agent placed in a random environment stagnates, while a routine following agent continues to improve. We can infer from this that object-shifting behaviors can be learned in a dynamic environment with routine-following placement behavior, proving our condition for feasibility. Finally, we perform P-ObjectNav with an LLM-based agent, and infer that only commonsense knowledge-based navigation is insufficient for good performance. We enhance the LLM with a memory interface, and the drastic improvement in performance suggests the need for memory in agents to capture object-specific placement patterns in the environment for improved inference. Code, dataset and additional ablation experiments will be released and provided in the supplementary.

6 Limitations and Broader Impacts

As we introduce a new task involving portable objects, we encounter a few limitations. We currently perform analysis on individual modules for navigation and visual grounding. As such, errors in the navigation stage would not affect the grounding and vice versa. Coupling these experiments would provide a better sense of realism to the high-level policy learning task.

While we provide a theoretical guarantee that an optimal path for maximizing the number of portable objects found exists if the object placement follows a routine, we only consider show this for a simplified case of a fully connected graph. One interesting route is to consider habits of various frequencies to better model short-term, long-term, and seasonal habits.

Yet another interesting direction, is to combine generative modeling of images with 2D simulators such as Minigrid [11]. As high-level navigation involves sequential decision-making at nodes rather than low-level planning, we believe a 3D simulation environment is too computationally expensive while also being unnecessarily challenging to setup. As such, one direction to explore is that of a *generative 2D simulator* that could generate images to mimic human and dynamic obstacles at various viewpoints.

In terms of broader impact, we believe our work provides a strong foundation in establishing the ObjectNav task for non-stationary environments. As such, we believe it to have an impact on the Embodied AI community, in fostering a new direction of research for navigation in dynamic, human-centric environments.

References

1. AlDahak, A., Elnagar, A.: A practical pursuit-evasion algorithm: Detection and tracking. In: *Proceedings 2007 IEEE International Conference on Robotics and Automation*. pp. 343–348 (2007). <https://doi.org/10.1109/ROBOT.2007.363810>
2. Anderson, P., Chang, A., Chaplot, D.S., Dosovitskiy, A., Gupta, S., Koltun, V., Kosecka, J., Malik, J., Mottaghi, R., Savva, M., et al.: On evaluation of embodied navigation agents. *arXiv preprint arXiv:1807.06757* (2018)
3. Batra, D., Gokaslan, A., Kembhavi, A., Maksymets, O., Mottaghi, R., Savva, M., Toshev, A., Wijmans, E.: Objectnav revisited: On evaluation of embodied agents navigating to objects. *arXiv preprint arXiv:2006.13171* (2020)
4. Cai, K., Wang, C., Cheng, J., De Silva, C.W., Meng, M.Q.H.: Mobile robot path planning in dynamic environments: A survey. *arXiv preprint arXiv:2006.14195* (2020)
5. Campari, T., Lamanna, L., Traverso, P., Serafini, L., Ballan, L.: Online learning of reusable abstract models for object goal navigation. In: *Proceedings of the IEEE/CVF Conference on Computer Vision and Pattern Recognition*. pp. 14870–14879 (2022)
6. Cancelli, E., Campari, T., Serafini, L., Chang, A.X., Ballan, L.: Exploiting proximity-aware tasks for embodied social navigation. In: *Proceedings of the IEEE/CVF International Conference on Computer Vision*. pp. 10957–10967 (2023)
7. Chang, A., Dai, A., Funkhouser, T., Halber, M., Niessner, M., Savva, M., Song, S., Zeng, A., Zhang, Y.: Matterport3d: Learning from rgb-d data in indoor environments. *arXiv preprint arXiv:1709.06158* (2017)
8. Chen, C., Al-Halah, Z., Grauman, K.: Semantic audio-visual navigation. In: *Proceedings of the IEEE/CVF Conference on Computer Vision and Pattern Recognition*. pp. 15516–15525 (2021)
9. Chen, C., Jain, U., Schissler, C., Gari, S.V.A., Al-Halah, Z., Ithapu, V.K., Robinson, P., Grauman, K.: Soundspaces: Audio-visual navigation in 3d environments. In: *Computer Vision–ECCV 2020: 16th European Conference, Glasgow, UK, August 23–28, 2020, Proceedings, Part VI* 16. pp. 17–36. Springer (2020)
10. Chen, K., Chen, J.K., Chuang, J., Vázquez, M., Savarese, S.: Topological planning with transformers for vision-and-language navigation. In: *Proceedings of the IEEE/CVF Conference on Computer Vision and Pattern Recognition*. pp. 11276–11286 (2021)
11. Chevalier-Boisvert, M., Dai, B., Towers, M., de Lazcano, R., Willems, L., Lahlou, S., Pal, S., Castro, P.S., Terry, J.: Minigrid & miniworld: Modular & customizable reinforcement learning environments for goal-oriented tasks. *CoRR abs/2306.13831* (2023)
12. Choi, Y., Oh, S.: Image-goal navigation via keypoint-based reinforcement learning. In: *2021 18th International Conference on Ubiquitous Robots (UR)*. pp. 18–21. IEEE (2021)
13. Clark, F., Sanders, K., Carlson, M., Blanche, E., Jackson, J.: Synthesis of habit theory. *OTJR: occupation, participation and health* **27**(1_suppl), 7S–23S (2007)
14. de Curtò, J., de Zarzà, I., Roig, G., Cano, J.C., Manzoni, P., Calafate, C.T.: Llm-informed multi-armed bandit strategies for non-stationary environments. *Electronics* **12**(13), 2814 (2023)
15. Deitke, M., Batra, D., Bisk, Y., Campari, T., Chang, A.X., Chaplot, D.S., Chen, C., D’Arpino, C.P., Ehsani, K., Farhadi, A., et al.: Retrospectives on the embodied ai workshop. *arXiv preprint arXiv:2210.06849* (2022)





16. Deitke, M., VanderBilt, E., Herrasti, A., Weihs, L., Salvador, J., Ehsani, K., Han, W., Kolve, E., Farhadi, A., Kembhavi, A., Mottaghi, R.: ProcTHOR: Large-Scale Embodied AI Using Procedural Generation (Jun 2022). <https://doi.org/10.48550/arXiv.2206.06994>
17. Deng, J., Dong, W., Socher, R., Li, L.J., Li, K., Fei-Fei, L.: ImageNet: A large-scale hierarchical image database. In: 2009 IEEE Conference on Computer Vision and Pattern Recognition. pp. 248–255 (Jun 2009). <https://doi.org/10.1109/CVPR.2009.5206848>
18. Dorbala, V.S., Mullen Jr, J.F., Manocha, D.: Can an embodied agent find your “cat-shaped mug”? llm-based zero-shot object navigation. *IEEE Robotics and Automation Letters* (2023)
19. Dorbala, V.S., Sigurdsson, G.A., Thomason, J., Piramuthu, R., Sukhatme, G.S.: Clip-nav: Using clip for zero-shot vision-and-language navigation. In: Workshop on Language and Robotics at CoRL 2022 (2022)
20. Gadre, S.Y., Wortsman, M., Ilharco, G., Schmidt, L., Song, S.: Clip on wheels: Zero-shot object navigation as object localization and exploration. *arXiv preprint arXiv:2203.10421* (2022)
21. Gadre, S.Y., Wortsman, M., Ilharco, G., Schmidt, L., Song, S.: Cows on pasture: Baselines and benchmarks for language-driven zero-shot object navigation. In: Proceedings of the IEEE/CVF Conference on Computer Vision and Pattern Recognition. pp. 23171–23181 (2023)
22. Guan, T., Yang, Y., Cheng, H., Lin, M., Kim, R., Madhivanan, R., Sen, A., Manocha, D.: Loc-zson: Language-driven object-centric zero-shot object retrieval and navigation (2023)
23. Gupta, A., Dollar, P., Girshick, R.: Lvis: A dataset for large vocabulary instance segmentation. In: Proceedings of the IEEE/CVF Conference on Computer Vision and Pattern Recognition (CVPR) (June 2019)
24. Jocher, G., Chaurasia, A., Qiu, J.: Ultralytics YOLO (Jan 2023), <https://github.com/ultralytics/ultralytics>
25. Kirillov, A., Mintun, E., Ravi, N., Mao, H., Rolland, C., Gustafson, L., Xiao, T., Whitehead, S., Berg, A.C., Lo, W.Y., Dollár, P., Girshick, R.: Segment anything (2023)
26. Krantz, J., Lee, S., Malik, J., Batra, D., Chaplot, D.S.: Instance-specific image goal navigation: Training embodied agents to find object instances. *arXiv preprint arXiv:2211.15876* (2022)
27. Labadze, L., Grigolia, M., Machaidze, L.: Role of ai chatbots in education: systematic literature review. *International Journal of Educational Technology in Higher Education* **20**(1), 56 (2023)
28. Li, L.H., Zhang, P., Zhang, H., Yang, J., Li, C., Zhong, Y., Wang, L., Yuan, L., Zhang, L., Hwang, J.N., Chang, K.W., Gao, J.: Grounded Language-Image Pre-training (Jun 2022). <https://doi.org/10.48550/arXiv.2112.03857>
29. Li, W., Hong, R., Shen, J., Yuan, L., Lu, Y.: Transformer memory for interactive visual navigation in cluttered environments. *IEEE Robotics and Automation Letters* **8**(3), 1731–1738 (2023). <https://doi.org/10.1109/LRA.2023.3241803>
30. Liang, Y., Chen, B., Song, S.: Sscnav: Confidence-aware semantic scene completion for visual semantic navigation. In: 2021 IEEE international conference on robotics and automation (ICRA). pp. 13194–13200. IEEE (2021)
31. Lin, T.Y., Maire, M., Belongie, S.J., Hays, J., Perona, P., Ramanan, D., Dollár, P., Zitnick, C.L.: Microsoft coco: Common objects in context. In: European Conference on Computer Vision (2014), <https://api.semanticscholar.org/CorpusID:14113767>

32. Liu, S., Zeng, Z., Ren, T., Li, F., Zhang, H., Yang, J., Li, C., Yang, J., Su, H., Zhu, J., et al.: Grounding dino: Marrying dino with grounded pre-training for open-set object detection. *arXiv preprint arXiv:2303.05499* (2023)
33. Mavrogiannis, C.I., Knepper, R.A.: Decentralized multi-agent navigation planning with braids. In: *Algorithmic Foundations of Robotics XII: Proceedings of the Twelfth Workshop on the Algorithmic Foundations of Robotics*. pp. 880–895. Springer (2020)
34. Mohanan, M., Salgoankar, A.: A survey of robotic motion planning in dynamic environments. *Robotics and Autonomous Systems* **100**, 171–185 (2018). <https://doi.org/https://doi.org/10.1016/j.robot.2017.10.011>, <https://www.sciencedirect.com/science/article/pii/S0921889017300313>
35. Morris, T., Dayoub, F., Corke, P., Wyeth, G., Upcroft, B.: Multiple map hypotheses for planning and navigating in non-stationary environments. In: *2014 IEEE international conference on robotics and automation (ICRA)*. pp. 2765–2770. IEEE (2014)
36. Puig, X., Undersander, E., Szot, A., Cote, M.D., Yang, T.Y., Partsey, R., Desai, R., Clegg, A.W., Hlavac, M., Min, S.Y., et al.: Habitat 3.0: A co-habitat for humans, avatars and robots. *arXiv preprint arXiv:2310.13724* (2023)
37. Ramakrishnan, S.K., Gokaslan, A., Wijmans, E., Maksymets, O., Clegg, A., Turner, J., Undersander, E., Galuba, W., Westbury, A., Chang, A.X., et al.: Habitat-matterport 3d dataset (hm3d): 1000 large-scale 3d environments for embodied ai. *arXiv preprint arXiv:2109.08238* (2021)
38. Ramakrishnan, S.K., Chaplot, D.S., Al-Halah, Z., Malik, J., Grauman, K.: Poni: Potential functions for objectgoal navigation with interaction-free learning. In: *Proceedings of the IEEE/CVF Conference on Computer Vision and Pattern Recognition*. pp. 18890–18900 (2022)
39. Ramrakhya, R., Batra, D., Wijmans, E., Das, A.: Pirlnav: Pretraining with imitation and rl finetuning for objectnav. In: *Proceedings of the IEEE/CVF Conference on Computer Vision and Pattern Recognition*. pp. 17896–17906 (2023)
40. Ramrakhya, R., Undersander, E., Batra, D., Das, A.: Habitat-web: Learning embodied object-search strategies from human demonstrations at scale. In: *Proceedings of the IEEE/CVF Conference on Computer Vision and Pattern Recognition*. pp. 5173–5183 (2022)
41. Raychaudhuri, S., Campari, T., Jain, U., Savva, M., Chang, A.X.: Mopa: Modular object navigation with pointgoal agents. In: *Proceedings of the IEEE/CVF Winter Conference on Applications of Computer Vision*. pp. 5763–5773 (2024)
42. Rudra, S., Goel, S., Santara, A., Gentile, C., Perron, L., Xia, F., Sindhwani, V., Parada, C., Aggarwal, G.: A contextual bandit approach for learning to plan in environments with probabilistic goal configurations. In: *2023 IEEE International Conference on Robotics and Automation (ICRA)*. pp. 5645–5652. IEEE (2023)
43. Sathyaamoorthy, A.J., Liang, J., Patel, U., Guan, T., Chandra, R., Manocha, D.: Densecavoid: Real-time navigation in dense crowds using anticipatory behaviors. In: *2020 IEEE International Conference on Robotics and Automation (ICRA)*. pp. 11345–11352. IEEE (2020)
44. Savva, M., Kadian, A., Maksymets, O., Zhao, Y., Wijmans, E., Jain, B., Straub, J., Liu, J., Koltun, V., Malik, J., Parikh, D., Batra, D.: Habitat: A Platform for Embodied AI Research (Nov 2019)
45. Shah, D., Eysenbach, B., Kahn, G., Rhinehart, N., Levine, S.: Ving: Learning open-world navigation with visual goals. In: *2021 IEEE International Conference on Robotics and Automation (ICRA)*. pp. 13215–13222. IEEE (2021)

46. Stiffler, N.M., O’Kane, J.M.: Planning for robust visibility-based pursuit-evasion. In: 2020 IEEE/RSJ International Conference on Intelligent Robots and Systems (IROS). pp. 6641–6648 (2020). <https://doi.org/10.1109/IROS45743.2020.9341031>
47. Vladareanu, V., Tont, G., Vladareanu, L., Smarandache, F.: The navigation of mobile robots in non-stationary and non-structured environments. *International Journal of Advanced Mechatronic Systems* **5**(4), 232–242 (2013)
48. Wu, Q., Wang, J., Liang, J., Gong, X., Manocha, D.: Image-goal navigation in complex environments via modular learning. *IEEE Robotics and Automation Letters* **7**(3), 6902–6909 (2022)
49. Yadav, K., Ramrakhya, R., Ramakrishnan, S.K., Gervet, T., Turner, J., Gokaslan, A., Maestre, N., Chang, A.X., Batra, D., Savva, M., et al.: Habitat-matterport 3d semantics dataset. In: *Proceedings of the IEEE/CVF Conference on Computer Vision and Pattern Recognition*. pp. 4927–4936 (2023)
50. Yokoyama, N.H., Ha, S., Batra, D., Wang, J., Bucher, B.: Vlfm: Vision-language frontier maps for zero-shot semantic navigation. In: *2nd Workshop on Language and Robot Learning: Language as Grounding* (2023)
51. Yu, B., Kasaei, H., Cao, M.: L3mvn: Leveraging large language models for visual target navigation. In: 2023 IEEE/RSJ International Conference on Intelligent Robots and Systems (IROS). IEEE (Oct 2023). <https://doi.org/10.1109/iros55552.2023.10342512>, <http://dx.doi.org/10.1109/IROS55552.2023.10342512>
52. Zhai, A.J., Wang, S.: Peanut: predicting and navigating to unseen targets. In: *Proceedings of the IEEE/CVF International Conference on Computer Vision*. pp. 10926–10935 (2023)
53. Zhao, X., Ding, W., An, Y., Du, Y., Yu, T., Li, M., Tang, M., Wang, J.: Fast segment anything (2023)
54. Zhao, X., Ding, W., An, Y., Du, Y., Yu, T., Li, M., Tang, M., Wang, J.: Fast segment anything. *arXiv preprint arXiv:2306.12156* (2023)
55. Zheng, Y., Meng, Z., Hao, J., Zhang, Z., Yang, T., Fan, C.: A deep bayesian policy reuse approach against non-stationary agents. *Advances in neural information processing systems* **31** (2018)
56. Zhou, G., Hong, Y., Wu, Q.: Navgpt: Explicit reasoning in vision-and-language navigation with large language models (2023)
57. Zhou, K., Zheng, K., Pryor, C., Shen, Y., Jin, H., Getoor, L., Wang, X.E.: Esc: Exploration with soft commonsense constraints for zero-shot object navigation. *arXiv preprint arXiv:2301.13166* (2023)
58. Zhou, Y., Ho, H.W.: Online robot guidance and navigation in non-stationary environment with hybrid hierarchical reinforcement learning. *Engineering Applications of Artificial Intelligence* **114**, 105152 (2022)

Supplementary Material

Right Place, Right Time!

Vishnu Sashank Dorbala^{*1}  Bhrij Patel^{*1}  Amrit Singh Bedi²  and Dinesh Manocha¹ 

University of Maryland, College Park MD 20740, USA

1 P-ObjectNav Definition

The objective of ObjectNav as defined in literature [2] is to literature to navigate to a target object specified by a target label in a previously unseen environment. Prior techniques [4, 5, 9] for solving this can be broadly broken down into two components 1) Sequential Decision Making and 2) Visual Grounding. The latter decides how the agent should navigate at each waypoint, while the former decides where in the final image the target object lies in. Our work introduces **two key changes** to this setup -

1. We add spatial and temporal dynamism to embodied environment.
2. There is no singular intended target per episode ("Get to the chair", for example), but rather the task is to find as many portable targets as possible within the episode.

Formally, we can define P-ObjectNav as "*Finding and visually grounding the most number of portable objects possible within a fixed period of timesteps in a dynamic environment.*"

Elaborating further on what was mentioned in the Formulation section — to maximize finding portable objects across n timesteps, we need to solve for an optimal subgraph $G_o \subset G$ covering most objects. Here, $G = (V, E)$, where V is a vertex set containing a distribution of portable objects, and E is the edge set containing distances between the vertices. The positions of V and E remain fixed over time, and the only changing value is portable object distribution.

If $G_i \subset G$ over t timesteps represents the unique subgraph obtained in the i th episode by an exploratory agent, and $G' \subset G$ over the same t timesteps represents the evolution of portable objects over the same set of nodes, our objective is to maximize the intersection between both these graphs to give us G_o . P-ObjectNav in this context can be considered a **Temporal Subgraph Optimization Problem**, that aims to optimize for maximizing the value sum (number of portable objects found) over a subgraph evolving over time t .

An alternate way to think of this is as an open-loop travelling salesperson problem (TSP), being optimized on maximizing the *loot* (or reward) obtained over a fixed set of timesteps, as opposed to minimizing loop distance.

Clarification on Feasibility As defined previously, our objective with P-ObjectNav is to maximize the number of portable target objects found over a

fixed set of timesteps. If these objects keep shifting randomly, the maximization objective would not be verifiable, as $\sum G_o$ representing the number of portable objects found would have a high variance. As such, in order for our task to be *feasible*, i.e., have a **ground truth maximum** on the number of objects that can be found over a fixed timespan, our hypothesis is that the objects themselves cannot be placed in random, but instead must follow a fixed routine. We use this hypothesis to derive Equation 3, and our objective in regards to proving task feasibility is to experimentally verify this statement.

2 Dataset Details

While the P-ObjectNav agents introduced in Section 2 tackle the *temporal* dynamism, i.e., identifying *where* and *when* the target object is likely to lie at a particular location, visual grounding is a separate task tackling *spatial* dynamism. An ideal agent performs both these tasks *simultaneously*, verifying at each timestep if a portable target exists by running a grounding model. As navigation decisions are not directly impacted by the performance of a grounding model, we study temporal and spatial dynamism independently.

The P-ObjectNav dataset contains temporal and spatial modifications on the Matterport3D scans. Further, we provide code and useful tools for implementing these modifications.

For temporal placement, we provide 6 dictionaries, two for each case i.e., *Random*, *Semi-Routine* and *Routine* object placement scenarios. For each case, one dictionary contains a mapping of Matterport3D nodes to Portable Objects (according to Table 1) and the other dictionary contains a mapping of the Portable Objects to Timestamps for when they lie at those nodes.

For the spatial placement, we provide a dataset of 10,500 modified images taken across 10 randomly chosen Matterport3D scans, with 21 portable objects randomly oriented and positioned 5 times within each image. To emulate realism such that the portable objects are not floating in the sky or on the ceiling, they are placed on a large segmented area below the center of the image. We also provide the bounding boxes pertaining to the portable object in each image.

2.1 Temporal: Implementing Object Placement Strategies

In this section, we give more details on how we implemented the dynamic Matterport3D environment for training the PPO agent and for inference with LGX.

Matterport3D Modifications :

Each Matterport3D (MP3D) scan represents a household environment consisting of a set of panoramic view points. Along with the viewpoints (or nodes), we are also given the exact 3D position as well as the relative distance between them. For modifying the MP3D environment, we first construct topological graphs of each scan, with nodes containing the position and the panoramic image, and edges containing relative distance between them. We consider 10

different scans chosen from the REVERIE [8] and R2R [1] unseen validation splits for inference. We choose scans according to these datasets as they contain a variety of rooms for us to populate (Refer Table 1 in the main paper).

The nodes of the topological graphs are then updated at each timestep with the portable objects according to the object placement scenario that has been chosen.

Strategy Overview :

We save the precomputed trajectories of each episode described in Section 3.2 as two dictionaries: “object timesteps” and “object nodes”. Both dictionaries have the same keys, the portable object names. In “object timesteps”, the value associated with each key is the list of random intervals of timesteps that partition the total timesteps. In “object nodes”, the values are a list of node IDs. The node ID at index i for portable object p in “object nodes” corresponds to the interval at index i for portable object p in “object timesteps”. This relationship means that portable object p is at that particular node ID and that time interval.

When the agent reaches a node in the environment, we need to check which portable objects, if any, are in that node. For each portable object, we take the current timesteps and find the index of the time interval where it falls within. We then check the node ID at that index in “object nodes” to see if it matches the node ID of the current node. If so, we append the portable object to a list of found portable objects. After scanning through the dictionaries of each portable object, we then return the list of found portable objects to calculate the reward for PPO training or feedback to the LLM in LGX.

For example, say “mug” has the following random partition and node placement sequences:

$$(1, 10), (11, 32), (33, 44), (45, 50)$$

$$\text{NodeA}, \text{NodeB}, \text{NodeA}, \text{NodeC}$$

Then at timestep 47, it will scan the partition and see that 125 falls within the fourth interval and the corresponding node is NodeC. If the agent is at NodeC, then “mug” would be added to the found object list. We like to highlight the ease of adding more data if needed. If we would like to expand the number of timesteps of the episode to say 1000, we can simply make a random partition from 51 to 1000 and then sample a node for each new interval created.

Fully-Routine vs Semi-Routine vs Random: For random, for each time interval, the portable object is allowed to go to any room. For fully-routine and semi-routine, the object can only choose from rooms as described in Table 1 of the main body of the paper. For each episode, we create a new partition and placement sequence dictionaries, seeded by the episode number, and store those dictionaries in a file. For fully-routine, since the object path is constant throughout episodes, no matter the episode, we always choose the first episode dictionaries to determine the object trajectories. For semi-random, we choose the dictionaries whose seeds correspond to the episode number.

2.2 Spatial: Implementing Visual Grounding

In this section, we talk about our strategy for spatial placement of multiple portable target objects on MP3D scenes. After placing portable objects at various locations, we perform visual grounding using three Open-World Object Detection models for inference.

Generating Spatial Data :

We randomly choose 100 skybox images taken across the 10 MP3D scans mentioned in the previous subsection. While selecting these images are not of the ceiling or the floor, and have objects pertaining everyday scenes. We then pick stock images of all the 21 portable objects present in Table 1 of the main manuscript. These images are shown in Figure 6.



Fig. 1: OWL-ViT Detection Failures: Note the poor detection accuracy of OWL-ViT. On both images, it completely misses the object when prompted with a text containing the target label. We attribute these failures to unnatural images being generated by pasting target objects onto the scene.

For each of the skybox images, we first run FastSAM [10] and segment out the largest regions below the center of the image. We then randomly orient the portable object and place it at a random position on one of these segments. Choosing segments below the center of the image is necessary to ensure that the portable objects being placed follow commonsense, and do not hang in the ceiling. This is done 5 times for each of the 21 objects on 100 images, to get 10500 images in total. While placing the images, we also store the boundaries of the overlay as the ground truth bounding box for computing Intersection over Union (IOU) scores.

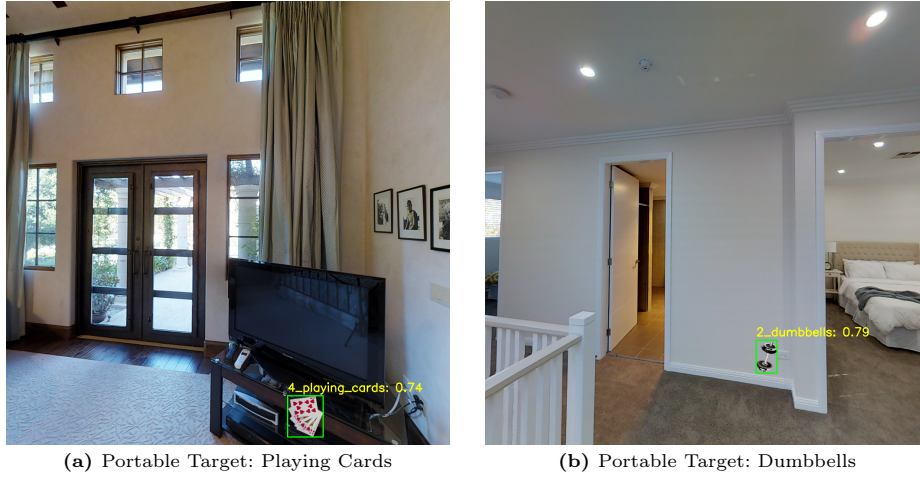


Fig. 2: GLIP Detection Accuracy: Note the superior detection accuracy, despite the low coverage on GLIP. On the image on the left and right, playing cards and dumbbells are detected correctly with a high accuracy.

Examples of this generated data is shown in Figure 4. Note that the same image can have multiple target segmentations (*bed* and *cushion* for example), with different objects placed on them at different orientations.

Open-World Visual Object Grounding We perform Visual Grounding on the spatial placement dataset using various Open-Vocabulary Object Detection Models. For each model, we assess the **Detection Coverage**, which is the percentage of images where the portable object was found, the **Detection Accuracy**, the accuracy of the predicted detections, and finally **Mean IOU**, which gives us the overlap between the ground truth bounding box of the placed target and the predicted box. The results for this are shown in Table 1.

Approach	Detection Coverage	Detection Accuracy	MIOU
OWL-ViT [7]	100%	3.04%	0.352
GLIP [6]	7.11%	100%	0.489
YOLO-World [3]	32.94%	0.2%	0.130

Table 1: Comparison of Open-World Object Detection Approaches

We make some interesting observations. OWL-ViT [7] outperforms GLIP [6] and YOLO-World [3] when it comes to Detection Coverage, which means that it consistently detects an object, irrespective of whether it is right or wrong on the



Fig. 3: YOLO Detection Failures: Note the poor detection accuracy of YOLO. On the image on the left, the screwdriver is grounded correctly, but the object name predicted is “Cow”. On the image on the right, YOLO completely misses the target object toothbrush, and instead grounds and labels something else.

image. This is evident since it takes a target object label is given as a prompt to OWL-ViT, so it detects something in the image, even if the confidence is low. Figure 1 shows some examples of this.

GLIP, while having lower detection coverage, has a perfect detection accuracy, meaning that when GLIP does detect something, it usually is correct. The high MIOU score associated with GLIP also corroborates with this fact. Figure 2 shows some example results of this.

We infer the YOLO-World model with custom vocabulary consisting of all the portable object names. Despite this, YOLO still performs the worst among the three, with poor detection accuracy and coverage. Figure 3 showcases one of these results. Notice that in the first image screwdriver is grounded at the right location, but the label is “Cow”. In the second image, both the predicted target (fire hydrant) and the grounding is wrong.

We note that the poor detection as measured by MIOU could be a result of unnatural scenes that are different from those which these models might have been trained on. Beyond this, grounding small, portable targets that could be present on various surfaces in a household environment still remains a challenge. We will be releasing this dataset to foster research in this area.

3 Heatmap Visualizations

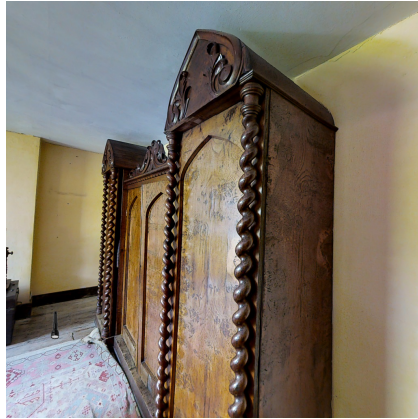
To better analyze the camping behavior of the agent, we visualize the node visitation distribution of the agent of the last episode. In Figure 7 the left column of images represents a heatmap of the nodes visited in the last episode of the



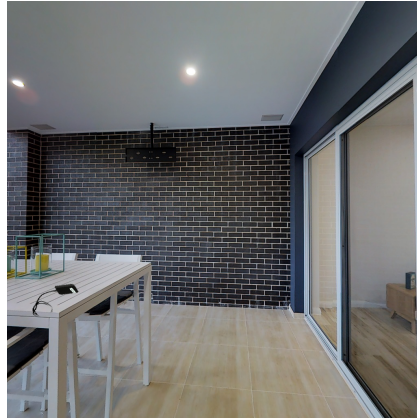
(a) Dice on Bed



(b) Mug on Cushion



(c) Flashlight on Floor

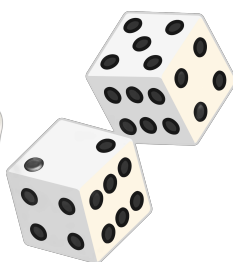


(d) Charger on Table

Fig. 4: Various Spatial Placement in our Dataset: Figures (a) and (b) look at different arrangements of objects in the same room. Figure (c) shows a flashlight on the floor, and figure (d) shows a charger on the table. We cover various orientations and rotations of portable objects being placed on various objects in different MP3D scans.



(a) bowl



(b) dice



(c) dumbbell



(d) flashlight



(e) glasses



(f) hat



(g) salt and pepper shakers



(h) screwdriver



(i) toothbrush



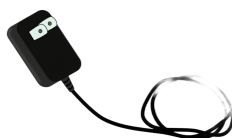
(j) remote



(k) playing cards



(l) phone



(m) phone charger



(n) notebook



(o) mug



Fig. 6: Portable Objects: A list of all the 21 portable objects we consider for our task.

agent, and the right column represents the object placement throughout the episode. The top row represents fully-routine movement. The middle row shows semi-routine object movement, and random movement is at the bottom. We see that semi-routine and fully-routine have the object at the same node throughout the episode. Upon further inspection, of all the possible rooms for “portable speaker”, the dining room is the only room present in the scan used to train PPO. Therefore, it makes sense that fully routine and semi-routine object placement distributions are the same as there is only one node possible. We also see that random placement, where “portable speaker” is allowed to go to any room in the scan, sits at the same node throughout the episode. Looking at the object time partition dictionary, we see that for random, the first interval in the sequence of partitions covers the first fifty timesteps. To avoid scenarios in the future, we believe that implementing a maximum partition length can help.

4 Temporal Object Placement Ablations

We train 2 more PPO agents in this ablation study where we progressively change the object movement scheme mid-training. In one training, we go from random movement to semi-routine after the first third of training, and then from semi-routine to fully-routine after the second third. In the second training, we go in the opposite direction from fully-routine to semi-routine to random. In Figure 8, we see that going to a more fixed object movement scheme (blue) causes

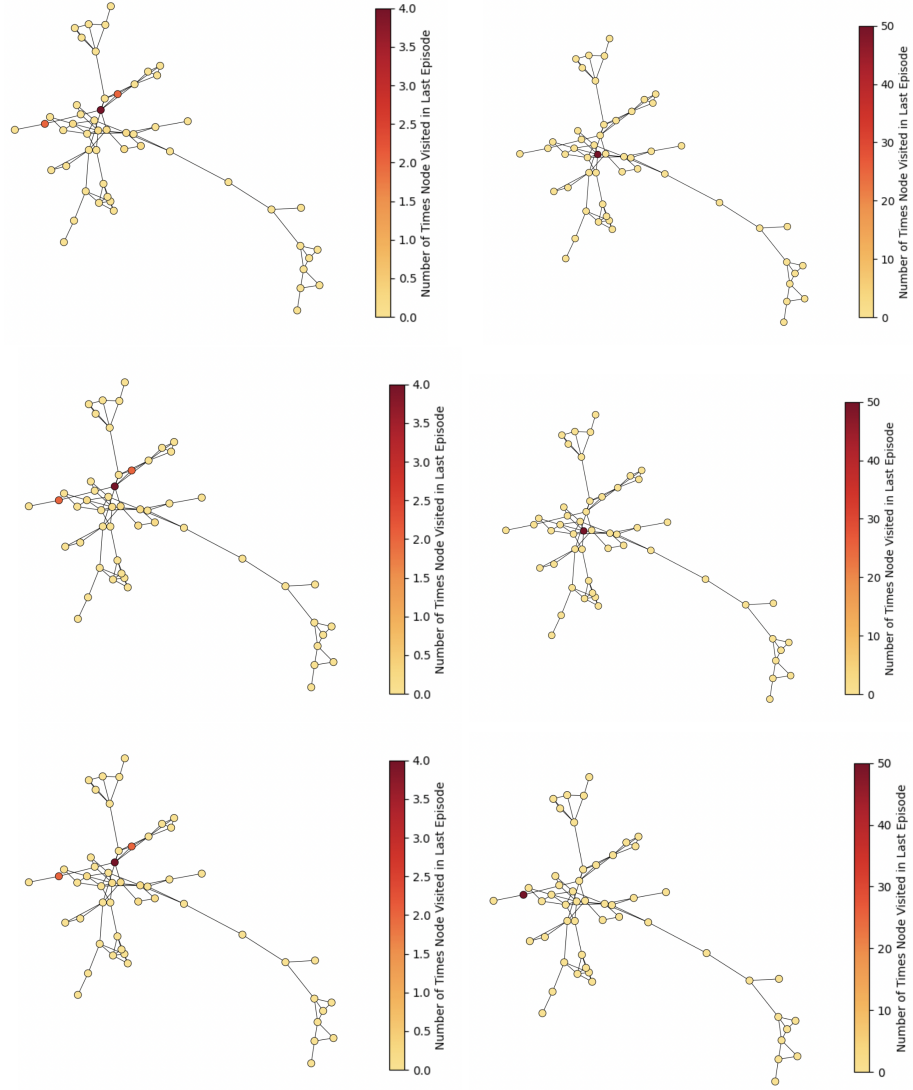


Fig. 7: Visualization of (left) Agent node visitation in the last episode and (right) “portable speaker” object placement in the last episode. (Top Row) Fully routine (Middle) Semi-Routine (Bottom) Random Placement.

the agent to find fewer objects over training while changing to a more random placement (orange) causes the agent to find more objects. Both trainings ran for 2000 episodes for 50 timesteps each.

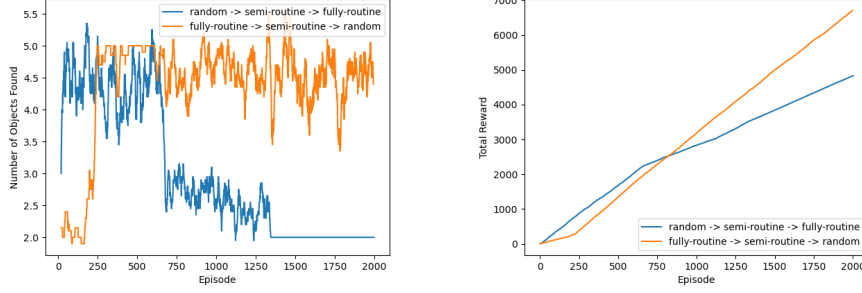


Fig. 8: (Left) Number of different portable objects at each episode and right) episode rewards. The blue curve represents going random to semi-routine to fully routine object movement and the orange curve represents going from fully routine to semi-routine to random.

5 Experimental Details

5.1 PPO Training

In this section, we reproduce for convenience the details of the PPO training from the main body:

Observations Space: We pass to the agent an $(n+1)$ -dimensional vector where n is the number of nodes in the Matterport3D scan. Each element except for the last one, contains a binary value where the value is only 1 if the node corresponding to that index is adjacent to the current and is 0 otherwise. The last element in the observation space is the timestep.

Action Space: Given a state vector from the observation space, the agent policy outputs an integer representing the index of the node in the observation space vector the agent will travel to next.

Reward Structure: For each transition in the environment, the agent receives a reward of +1 for every new portable object from Table ?? it finds. If the action a is an index corresponding to a node that is not adjacent to the current node, the agent receives a penalty of -1. Formally, let A be the set of adjacent nodes at timestep t , and let $P(t)$ be the set of new portable objects seen at t .

$$R(t) = |P(t)| - \mathbb{1}_{a \notin A} \quad (1)$$

For each object movement scheme, random, semi-routine, and fully routine, we train the PPO agent for 2000 episodes with 50 timesteps each. We use StableBaseline3 with neural network parameterizations of both policy and critic.

5.2 LGX Inference

We utilize the official implementation of LGX ¹ and incorporate it into our modified MP3D environment. Briefly, at each timestep, LGX scans the node for objects, and asks an LLM for directions to reach a target. In our case, we seek to maximize finding portable targets. As such, we prompt GPT-4 with the following base prompts -

System Prompt - "I am a smart robot trying to find as many portable objects as I can at home."

User Prompt - "Which object from $\langle OBJECT_LIST \rangle$ should I go towards to find a new portable object? Reply in ONE word."

The $\langle OBJECT_LIST \rangle$ here contains a set of objects that have been detected using YOLO-v8, as proposed in LGX. Additionally, we if a portable object is present at a certain node at a given timestep, we add it to this list.

The LLM then predicts a target object from the list, which is mapped to an adjacent node using our customized MP3D functions.

For the **memory-enhanced** agents, we slightly modify the System Prompt, based on what type of memory (complete or selective) was passed.

For *Complete*, we additionally ask -

System Prompt:

I have seen the following objects and taken the following actions so far -

1. $\langle OBJECT_LIST \rangle$: ACTION
2. $\langle OBJECT_LIST \rangle$: ACTION

...

User Prompt:

Which object from $\langle OBJECT_LIST \rangle$ should I go towards to find a new portable object? Reply in ONE word.

For the *Selective* case,

System Prompt:

I have found the following path (object chain) to a portable object from the current observation. It takes K timesteps -

1. $\langle P-Obj \rangle$: $\langle ACTION_TRACE \rangle$

User Prompt:

Should I follow the action traceback? Reply with YES/NO.

Note P-Obj here refers to Portable Object, and ACTION_TRACE refers to the object chain that was found in the MemoryTree for that portable object. K represents the length of the traceback on the tree.

If the LLM responds with YES, we execute the action traceback, and run forward K timesteps. If not, we stick to the base prompt.

¹ <https://github.com/vdorbala/LGX>

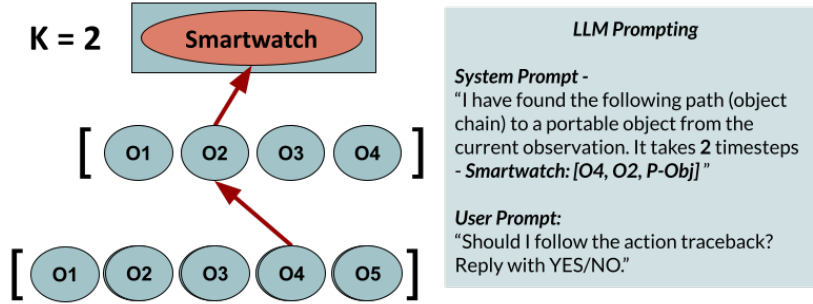


Fig. 9: MemoryTree: We interface the LLM’s system prompt with a Memory Tree. When a path to a portable target has been found in the tree, the LLM is shown the path, along with the cost ($K = 2$ in this image), and is asked whether or not it should follow the path. Note the portable target object is temporally moved, so by the time the agent gets to the target after K timesteps, there is a possibility that the object isn’t there anymore.

5.3 Memory Tree

In our Selective Memory approach, we interface a MemoryTree with the LLM to selectively pass appropriate information about the presence of portable objects. Each node of the MemoryTree contains a set of objects that the agent has seen at a particular timestep. Each object is its own node, and has leaf nodes associated with the objects that the agent would encounter if it chooses to pick that object. The LLM selects an object from a list of observations, and after hopping to that node, we populate the leaf node of that particular object.

During each timestep, we also perform BFS on the tree to search for the nearest possible portable object. Once a portable object has been found, the BFS search will always return true. However, note that as the objects are portable, they need not be at the same node as what was predicted by the tree. As such, we present the LLM with a choice of whether to follow or not follow the MemoryTree’s path. Additionally, if multiple paths are found, we only choose the once closest to the current observation to avoid overloading the LLM prompt. Refer to Figure 9 for an illustration.

6 Code and Dataset

We provide an anonymous link to our Code ². The dataset will be present as a downloadable link in the code repository.

² <https://anonymous.4open.science/r/PObjectNav-A981>

References

1. Anderson, P., Wu, Q., Teney, D., Bruce, J., Johnson, M., Sünderhauf, N., Reid, I., Gould, S., Van Den Hengel, A.: Vision-and-language navigation: Interpreting visually-grounded navigation instructions in real environments. In: Proceedings of the IEEE conference on computer vision and pattern recognition. pp. 3674–3683 (2018)
2. Batra, D., Gokaslan, A., Kembhavi, A., Maksymets, O., Mottaghi, R., Savva, M., Toshev, A., Wijmans, E.: Objectnav revisited: On evaluation of embodied agents navigating to objects. arXiv preprint arXiv:2006.13171 (2020)
3. Cheng, T., Song, L., Ge, Y., Liu, W., Wang, X., Shan, Y.: Yolo-world: Real-time open-vocabulary object detection (2024)
4. Dorbala, V.S., Mullen Jr, J.F., Manocha, D.: Can an embodied agent find your “cat-shaped mug”? llm-based zero-shot object navigation. IEEE Robotics and Automation Letters (2023)
5. Gadre, S.Y., Wortsman, M., Ilharco, G., Schmidt, L., Song, S.: Cows on pasture: Baselines and benchmarks for language-driven zero-shot object navigation. In: Proceedings of the IEEE/CVF Conference on Computer Vision and Pattern Recognition. pp. 23171–23181 (2023)
6. Li, L.H., Zhang, P., Zhang, H., Yang, J., Li, C., Zhong, Y., Wang, L., Yuan, L., Zhang, L., Hwang, J.N., Chang, K.W., Gao, J.: Grounded Language-Image Pre-training (Jun 2022). <https://doi.org/10.48550/arXiv.2112.03857>
7. Minderer, M., Gritsenko, A., Stone, A., Neumann, M., Weissenborn, D., Dosovitskiy, A., Mahendran, A., Arnab, A., Dehghani, M., Shen, Z., Wang, X., Zhai, X., Kipf, T., Houlsby, N.: Simple open-vocabulary object detection with vision transformers (2022)
8. Qi, Y., Wu, Q., Anderson, P., Wang, X., Wang, W.Y., Shen, C., van den Hengel, A.: REVERIE: Remote Embodied Visual Referring Expression in Real Indoor Environments (Jan 2020)
9. Yadav, K., Majumdar, A., Ramrakhya, R., Yokoyama, N., Baevski, A., Kira, Z., Maksymets, O., Batra, D.: Ovr1-v2: A simple state-of-art baseline for imagenav and objectnav. arXiv preprint arXiv:2303.07798 (2023)
10. Zhao, X., Ding, W., An, Y., Du, Y., Yu, T., Li, M., Tang, M., Wang, J.: Fast segment anything. arXiv preprint arXiv:2306.12156 (2023)